arXiv:cond-mat/0310274v3 [cond-mat.stat-mech] 25 Oct 2003

# Self-Organized Criticality in a Bulk Driven One-Dimensional Deterministic System [1]

Maria de Sousa Vieira [2]

*International Center for Complex Systems, Departamento de Fisica, UFRN,59072 970 Natal, RN, Brazil.*

**Abstract**

We introduce a deterministic self-organized critical system that is one dimensional and bulk driven. We find that there is no unique universality class associated with the system. That is, the critical exponents change as the parameters of the system are changed. This is in contrast with the boundary driven version of the model [M. de Sousa Vieira, *Phys. Rev. E* **61** (2000) 6056] in which the exponents are unique. This model can be seen as a discretized version of the conservative limit of the Burridge-Knopoff model for earthquakes.

*Key words:* Self-Organized Criticality; Earthquake models.

Bak, Tang and Wiesenfeld(1) introduced the concept of Self-Organized Criticality (SOC) to explain the ubiquity of scaling invariance in Nature. In systems that present SOC power-law distribution of event sizes, limited only by the system size, is observed without fining tuning of parameters.

One of the most well known scaling invariant distributions in Nature is the Gutenberg-Richter law(2), which refers to a power-law distribution of earthquake sizes. Earthquake models have been studied in connection with SOC, one of them being the Burridge-Knopoff(3) model. That model consists of a linear chain of blocks connected to each other via springs and each block is connected to an upper bar, which is pulled with constant velocity. The blocks are on a surface with friction. Events of several sizes are observed as the blocks are pulled. Carlson and Langer(4) showed that the distribution of events follows a power-law for small events. Larger events follow a different distribution. The critical event size that separates those two distributions does not depend

[1] In honor of Constantino Tsallis in the celebration of his 60th birthday.

[2] e-mail: mariav_us@yahoo.com.

on the system size. Since the power-law distribution is not limited by the system size, it implies that the Burridge-Knopoff model, in the nonconservative version studied by Carlson and Langer, does not present SOC. Another model for earthquakes, also introduced by Burridge and Knopoff(3), in which only the first block of the chain is pulled does present SOC. Such a model has been called the train model(5). A discretized version of the train model model governed by coupled map lattices (CML) was introduced in (6). In a CML the space variables are continuous and the time is discrete.

The aim of this paper is to show that a CML discretized version of the Burridge-Knopoff model, the one in which all the blocks are connected to an upper bar, does present SOC in the conservative limit. Such a discretization was performed by Nakanishi on the same model(7). However, in his studies that system did not present SOC, even in the conservative limit, due to a different relaxation function he used. We also show that the critical exponents vary with the parameters of the model. This is in contrast with the train model, which has a unique universality class. The universality class of the train model is the same as the one of the Oslo rice pile model(8). To our knowledge, this is the first SOC model to be introduced that is bulk driven, one-dimensional and deterministic. We believe that our model could also be applied for granular material in a quasi-one-dimensional rotating drum. The two-dimensional version of this model was studied in (9) and that model presents avalanche size distribution consistent with what is observed in sand experiments.

In our discretized version of the Burridge-Knopoff model each element (i.e., blocks) $i$ is characterized by a variable $f_i$, which we will call force, with $i = 1, ..., L$, and $L$ being the number of elements in the system. The dynamical evolution of the system is determined by the following algorithm:

(1) Start the system by defining random initial values for the variables $f_i$, so the they are below a chosen, fixed, threshold $f_{th}$.

(2) Find the element in the system that has the largest $f$, denoted here by $f_{max}$. Then update all the elements according to $f_i \mapsto f_i + f_{th} - f_{max}$.

(3) Check the forces in each element. If an element $i$ has $f_i \geq f_{th}$, update $f_i$ according to $f_i' = \phi(f_i - f_{th})$, where $\phi$ is a given nonlinear function. Increase the forces in its two nearest neighboring elements according to $f_{i\pm1}' = f_{i\pm1} + \alpha\Delta f/2$, where $\Delta f = f_i - f_i'$ and $\alpha$ determines the level of conservation.

(4) If $f_i' < f_{th}$ for all the elements, go to step (2) (the event has finished). Otherwise, go to step (3) (the event is still evolving).

Without losing generality one can choose $f_{th} = 1$. The functional form we use for $\phi$ is $\phi(x) = 1 - d - a[x]$ where $[x]$ denotes $x$ modulo $(1 - d)/a$, that is, a sawtooth function. However, we have tested other periodic functions, such as

a triangular wave, and found that the behavior we show here remains, that is, the results are robust, the essential ingredient being periodicity (not necessary a perfect one) for $\phi$. The motivation for choosing a periodic function is due to the fact that we observed that in the Burridge-Knopoff model, modeled by ordinary differential equations (ODEs), the force in a block after a not so small event can have any value that is smaller than the maximum static friction force. Also, in the train model governed by CML only a periodic function reproduces what is seen in the system governed by ODEs, that is, SOC(5; 6). Nakanishi(7) used for $\phi$ a decreasing function, but that is unrealistic in our view for comparison with the system governed by ODEs.

In our system, the parameter region in which SOC is found is $a > 1$ and $d << 1$. For $a < 1$ one observes that the earthquakes merge with each other and the blocks never stop (for a discussion of the physical meaning of $a$ and $d$ and why $a = 1$ represents an important boundary in such kind of models, see (6; 9)). For the case $d = 1$ the system is not SOC and corresponds to the one-dimensional version of the OFC model(10). There is a transition at an intermediate values of $d$, which seems to be around $d = 0.7$, from SOC to non SOC behavior. It is beyond the scope of this paper to study such a transition. We simulate the system using open boundary conditions and parallel update. The number of avalanches we use is $10^6$ when $d \geq 0.1$ and $10^7$ when $d < 0.1$.

Although the focus of this work is on the conservative case ($\alpha = 1$) we first show an example of event size distribution in the case of non conservation. We show in Fig.1(a) the frequency of events $P(s)$ as a function of the the event size $s$ when $\alpha = 0.9$. The qualitative behavior seen is the same observed in the model governed by ODEs(4), that is, a power-law distribution for small events and a bumpy distribution for larger events. We have found that the events that belong to the power-law region are the ones that do not probe the large discontinuities of the relaxation function $\Phi$. In other words, the only nonlinearity probed by a block whose force exceeds the threshold is a small discontinuity determined by $d$. We will be talking of this regime as the "almost linear" one. We have found a similar situation in the system governed by ODEs. There, the bumpy part of the distribution has the events that probe the nonlinear regime of the friction force.

From now on we concentrate on the conservative case, i.e, $\alpha = 1$. We show in Fig.1(b) a typical case of the avalanche distribution (solid line) in that regime. We have found that that distribution can be divided in two distinct distributions: one for the almost linear regime (short dashed line) and one for the strong nonlinear regime (long dashed line). Power-law distribution limited only by the system size (i.e. SOC) occurs only in the strong nonlinear regime. We are going to concentrate our attention to that case only.

We have plotted in Fig.2(a) the distribution of event sizes $P(s)$ for the events

Fig. 1. Distribution of event sizes for (a) $a = 3$, $d = 0.01$, $\alpha = 0.9$ with $L = 128$ (solid), $L = 256$ (dashed) and (b) $a = 4$, $d = 0.1$ and $\alpha = 1$.

Fig. 2. Distribution of event sizes for (a) varying $a$ and $d$ and keeping $L$ the same and (b) when $L = 128, 256, 512, 1024$ with $a$ and $d$ kept constant. In (c) we show the finite-size scaling data collapse using $\tau = 1.06$ and $D = 2.20$.

that are in the strong nonlinear regime for different values of $a$ and $d$. We see that $P(s) \sim s^{-\tau}$, which is characteristic of SOC systems. However, $\tau$ is not unique and vary with the system parameters. In Fig.2(b) we show $P(s)$ for different system sizes keeping $a$ and $d$ the same, and in Fig.2(c) we show the data collapse using the finite-size scaling ansatz for that set of parameters. We have noticed that the value of $\tau$ depends slightly on the system size, but converges to a given value as $L$ increases. This has been seen in the Zhang model(11). The authors of (11) found that for the Zhang model the linear relation $\tau(L) = \tau_\infty - const/L$ is obeyed. By extrapolating $L \to \infty$ one obtains the value of $\tau$ for an infinite lattice. We have found the same in our model, and this is shown in Fig.3(a) for different parameter values.

In many SOC models for sandpiles it has been observed that grains propagate as an unbiased random walker. This combined with a conservation law implies that $< s > \sim L^2$(12). In our model we have seen that this does not always occur. Instead, in the limit of large $L$, the relation $< s > \sim L^\mu$ with $\mu \leq 2$ is observed. This means that the avalanche propagation in this model occurs subdifusively in some regions of the parameter space. The largest avalanche size scales as $s_{max} \sim L^D$. We have found that $D$ does not vary with the parameter values, having a value of $D \approx 2.20$.

It is not difficult to show that $D$, $\mu$ and $\tau_\infty$ are related by $\mu = D(2 - \tau_\infty)$ (see for example (13) for a derivation when $\mu = 2$). Consequently, if $D$ is constant and $\tau$ varies with the parameter values, this implies that $\mu$ cannot be same for all the parameter values. This is what Fig. 3(b) shows. We have estimated the asymptotic value of $\mu$ via $\mu = (\log < s_{L=1024} > - \log < s_{L=512} >)/(\log(1024) - \log(512) >)$, and we found the following values: $\mu = 1.67, 1.78, 2.05, 1.94$, for

Fig. 3. (a) Exponent $\tau$ as a function of $L$ for (from top to bottom) ($a = 4$, $d = 0.02$), ($a = 4$, $d = 0.03$), ($a = 4$, $d = 0.1$), ($a = 2$, $d = 0.1$) and (b) average value of the avalanches $< s >$ as a function of $L$.

$(a = 4, d = 0.02)$, $(a = 4, d = 0.03)$, $(a = 4, d = 0.1)$, $(a = 2, d = 0.1)$, respectively. Inputting the values of $\mu$ in $\mu = D(2 - \tau_\infty)$ we can find $\tau_\infty$ and the values of $\tau_\infty$ obtained in this way are in good agreement with what is shown in Fig.3(a).

I thank Maya Paczuski for enlightening discussions.

## References

[1] P. Bak, C. Tang, and K. Wiesenfeld, *Phys. Rev. Lett.* **59** (1987) 381.
[2] B. Gutenberg and C. F. Richer, *Bull. Seismol. Soc. Am.* **32** (1942) 163.
[3] R. Burridge and L. Knopoff, *Bull. Seismol. Soc. Am.* **57** (1967) 341.
[4] J. M. Carlson and J. S. Langer, *Phys. Rev. Lett.* **62** (1989) 2632.
[5] M. de Sousa Vieira, *Phys. Rev. A* **46** (1992) 6288.
[6] M. de Sousa Vieira, *Phys. Rev. E* **61** (2000) 6056.
[7] H. Nakanishi, *Phys. Rev. A* **43** (1991) 6613.
[8] M. Paczuski and S. Boettcher, *Phys. Rev. Lett.* **77** (1996) 111.
[9] M. de Sousa Vieira, *Phys. Rev. E* **66** (2002) 051306.
[10] Z. Olami *et. al*, *Phys. Rev. Lett.* **8** (1992) 1244.
[11] S. Lübeck, *Phys. Rev. E* **56** (1997) 1590; A. Giacometti and A. Diaz-Guilera, *Phys. Rev. E* **58** (1998) 247.
[12] L. P. Kadanoff et al., *Phys. Rev. A* **39** (1989) 6524.
[13] H. Nakanishi and K. Sneppen, *Phys. Rev. E* **55** (1997) 4012.

Fig. 1

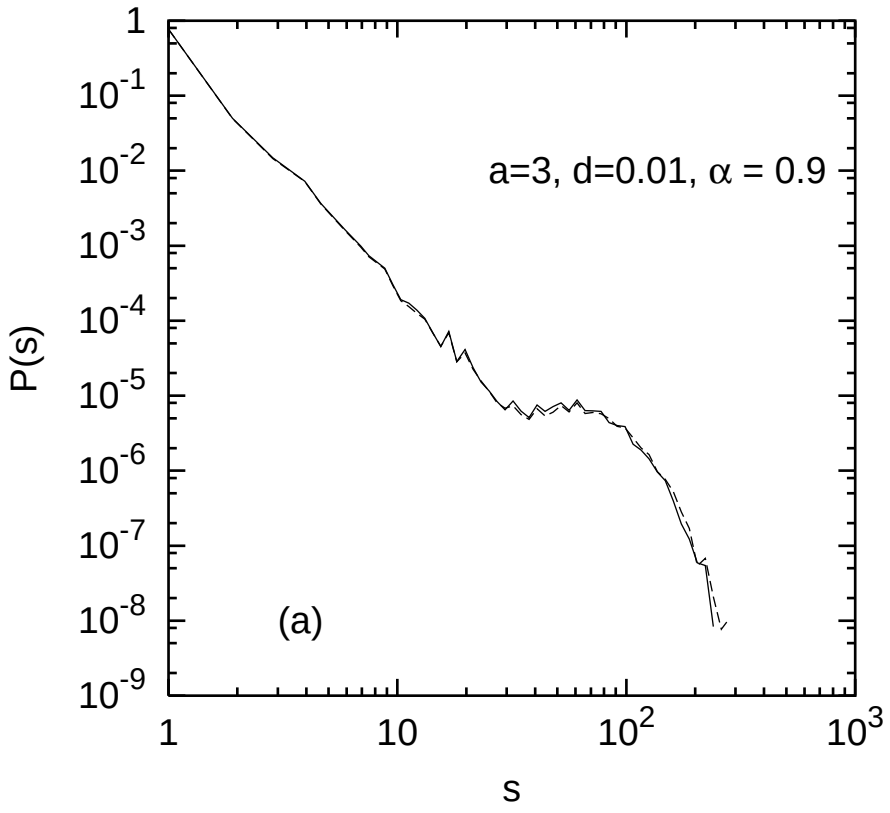
a=3, d=0.01, α = 0.9
(a)
P(s)
s
1
10^-1
10^-2
10^-3
10^-4
10^-5
10^-6
10^-7
10^-8
10^-9
1
10
10^2
10^3

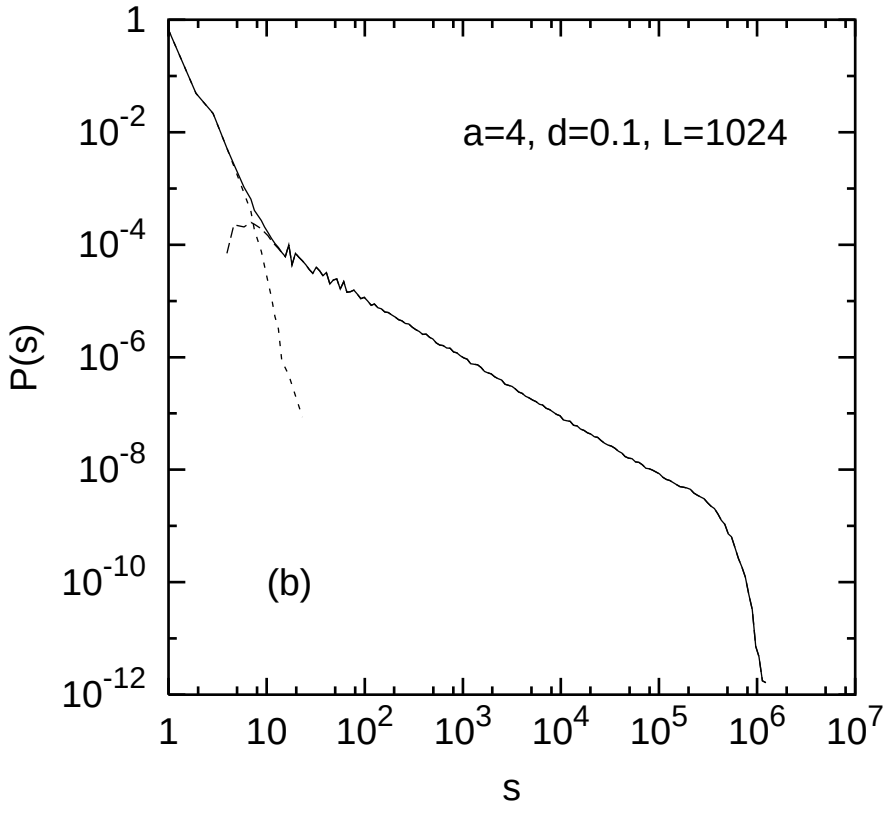
a=4, d=0.1, L=1024
(b)
P(s)
s
1
10^-2
10^-4
10^-6
10^-8
10^-10
10^-12
1
10
10^2
10^3
10^4
10^5
10^6
10^7

Fig. 2

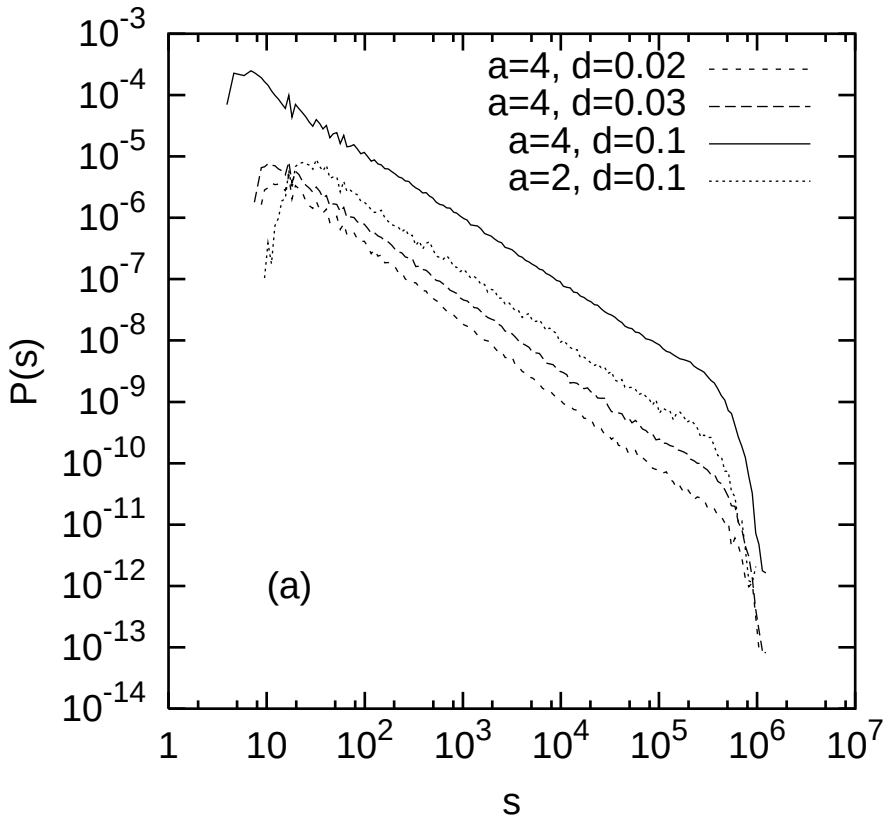


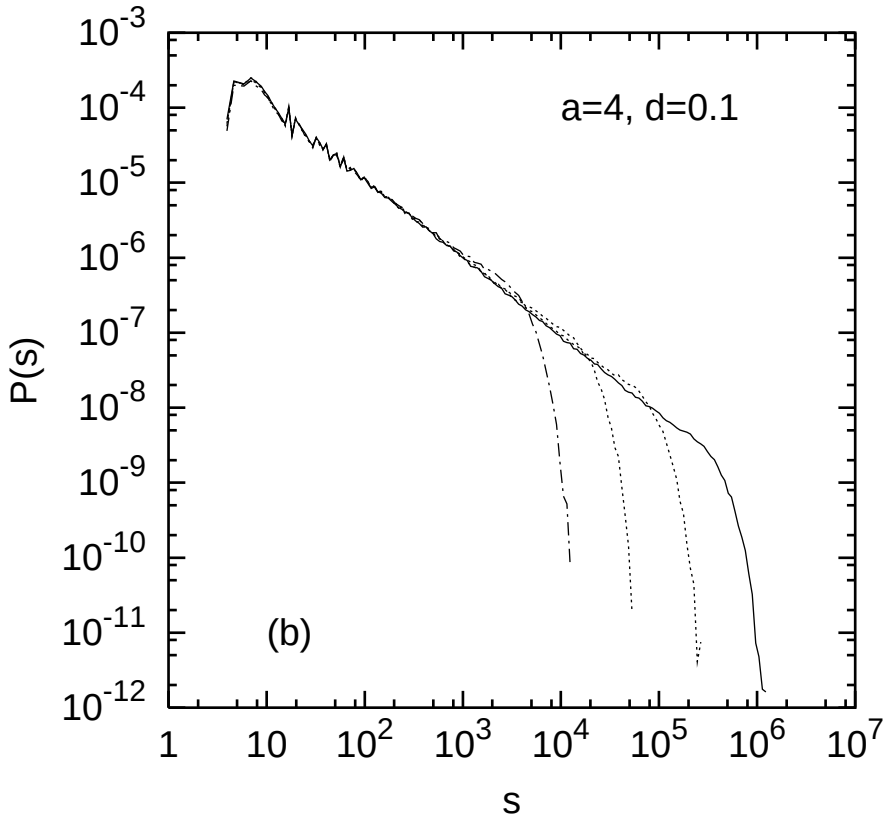

Fig. 2

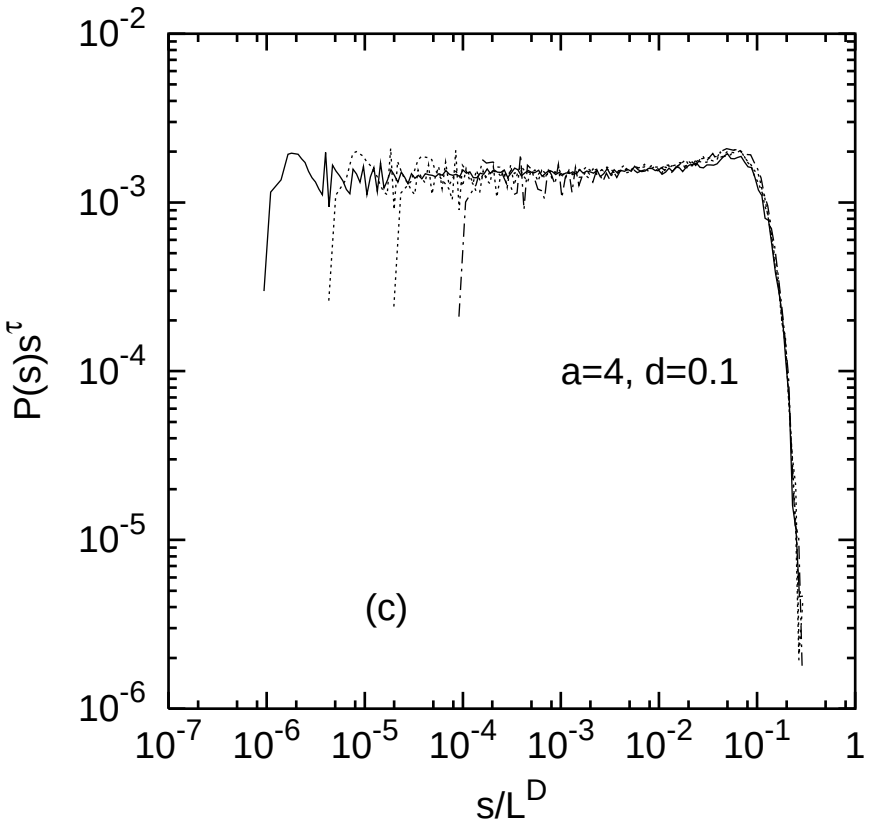
$10^{-2}$
$10^{-3}$
$10^{-4}$
$10^{-5}$
$10^{-6}$
$P(s)s^{\tau}$
a=4, d=0.1
(c)
$10^{-7}$
$10^{-6}$
$10^{-5}$
$10^{-4}$
$10^{-3}$
$10^{-2}$
$10^{-1}$
1
$s/L^{D}$

Fig. 3

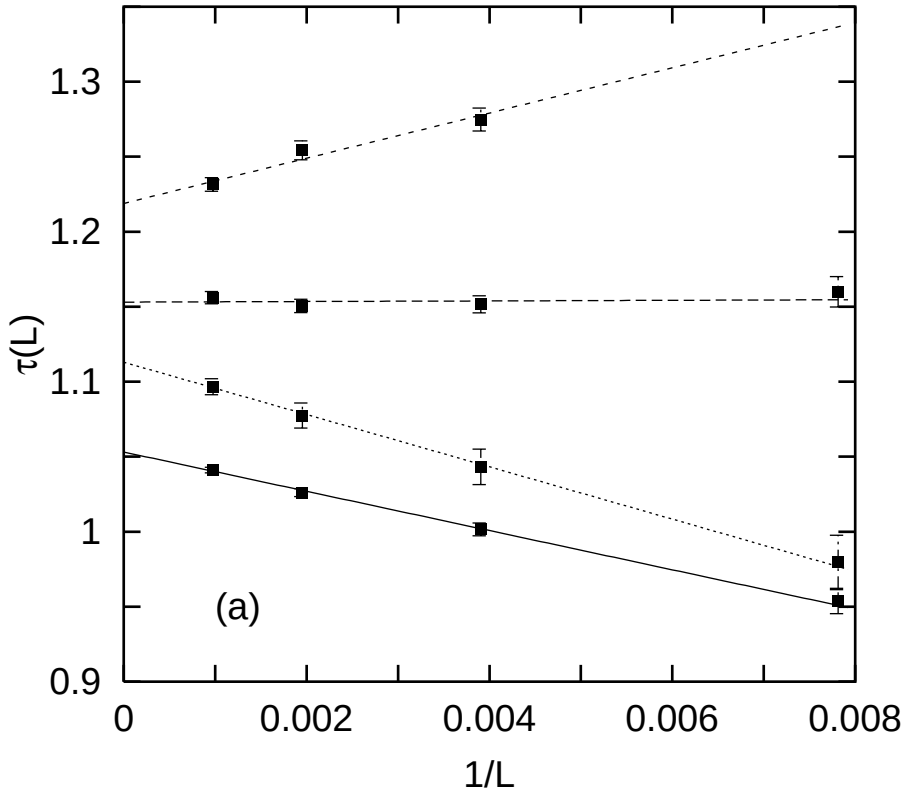
1.3
1.2
1.1
1
0.9
τ(L)
(a)
0
0.002
0.004
0.006
0.008
1/L

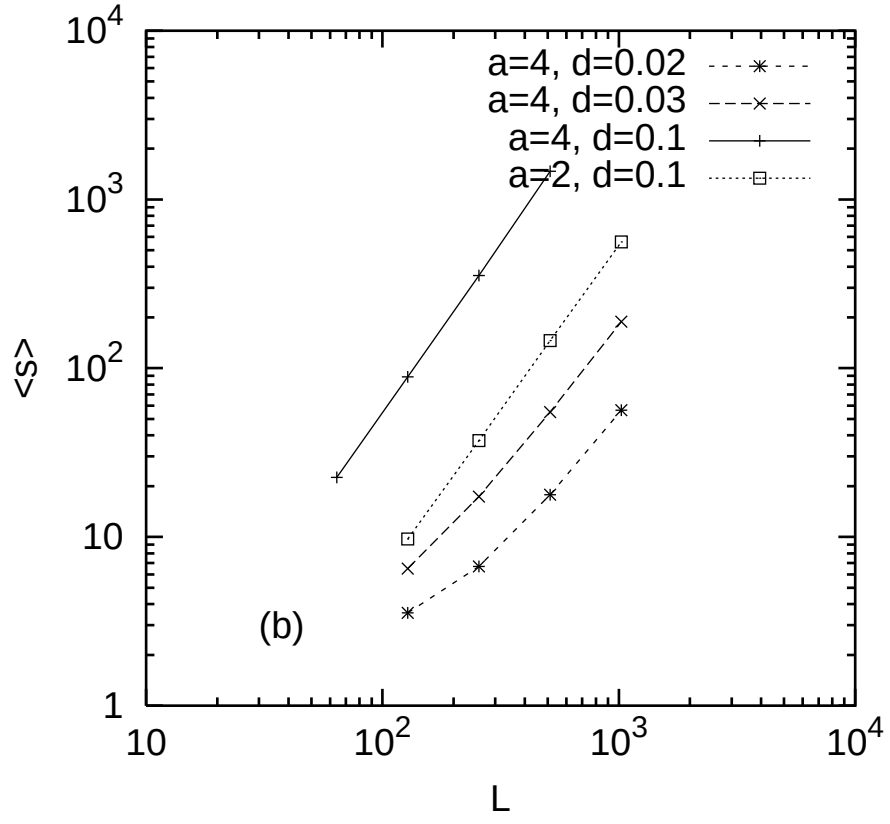
10^4
10^3
10^2
10
1
<s>
a=4, d=0.02
a=4, d=0.03
a=4, d=0.1
a=2, d=0.1
(b)
10
10^2
10^3
10^4
L